Werk

Jahr: 1980
Kollektion: fid.geo
Signatur: 8 Z NAT 2148:48
Digitalisiert: Niedersächsische Staats- und Universitätsbibliothek Göttingen
Werk Id: PPN1015067948_0048
PURL: http://resolver.sub.uni-goettingen.de/purl?PPN1015067948_0048

LOG Id: LOG_0036
LOG Titel: The solution of dynamic problems of elastic wave propagation on inhomogeneous media by a combination of partial separation of variables and finite-difference methods
LOG Typ: article

Übergeordnetes Werk

Werk Id: PPN1015067948
PURL: http://resolver.sub.uni-goettingen.de/purl?PPN1015067948
OPAC: http://opac.sub.uni-goettingen.de/DB=1/PPN?PPN=1015067948

Contact

Niedersächsische Staats- und Universitätsbibliothek Göttingen
Georg-August-Universität Göttingen
Platz der Göttinger Sieben 1
37073 Göttingen
Germany
Email: gdz@sub.uni-goettingen.de

J. Geophys. 48, 161–172, 1980

Journal of Geophysics

The Solution of Dynamic Problems of Elastic Wave Propagation in Inhomogeneous Media by a Combination of Partial Separation of Variables and Finite-Difference Methods*

A.S. Alekseev, B.G. Mikhailenko

Computing Center, Siberian Branch, Academy of Sciences of the USSR, Prospekt Nauki 6, 630090 Novosibirsk, USSR

Abstract. A new method for the calculation of theoretical seismograms, which is suitable for a wide class of inhomogeneous media, is suggested. The method is based on a combination of partial separation of variables with finite-difference techniques. Different variants of the method, based on the application of the Fourier-Bessel transform, finite integral transforms, expansions in Legendre polynomials, etc, are discussed in detail. Examples of theoretical seismograms for various simple structures are presented.

Key words: Theoretical seismograms – Finite differences – Partial separation of variables – Non-ray effects – Finite integral transforms.

1. Introduction

One of the basic problems of theoretical seismology and seismic prospecting is the computation of complete seismograms for inhomogeneous media. At present various methods can be used to compute theoretical seismograms. These methods have been applied successfully to the solution of many important problems in seismology. A brief review of these methods can be found in Červený et al. (1977). Most of these methods, however, give only incomplete theoretical seismograms, corresponding, to body waves or surface waves, for example. The most general method, at the present time, is the method of finite differences. The method is quite universal, but it is rather time consuming, and requires large amounts of computer store.

In this paper we will describe a new method for the calculation of theoretical seismograms, which is suitable for a wide class of inhomogeneous media, including vertically inhomogeneous media with block structures. The method is based on the combination of separation of variables with finite difference techniques. The basic principle of the method is the separation of the spatial variables (e.g., the coordinate corresponding to the epicentral distance). After this separation, the equation has reduced dimensionality, but remains hyperbolic. This equation can then be solved efficiently by finite differences.

We start with the application of this method to a vertically inhomogeneous halfspace and then proceed to more complicated cases.

* Presented at the Workshop Meeting on Seismic Waves in Laterally Inhomogeneous Media, Liblice, ČSSR, 27 February–3 March, 1978

2. Method of Solution

2.1. *Vertically Inhomogeneous Halfspace (Lamb's Problem)*

The physical problem that we are going to solve is the following: to determine the motion of the free surface and the interior of an inhomogeneous halfspace when a source of the normal-force type is located on the free surface. Since the geometry of the system has axial symmetry, it is convenient to use cylindrical coordinates (r, z).

The equation of motion of an inhomogeneous elastic medium is given by

$$(\lambda+2\mu)\,\mathrm{grad}\,\mathbf{U}-\mu\,\mathrm{rot}\,\mathrm{rot}\,\mathbf{U}+\mathrm{div}\,\mathbf{U}\,\mathrm{grad}\,\lambda +2(\mathrm{grad}\,\mu\cdot E)=\rho\frac{\partial^2\mathbf{U}}{\partial t^2}, \tag{1}$$

with the boundary conditions

$$\tau_{zz}|_{z=0}=-f(t)\,r^{-1}\,\delta(r), \qquad \tau_{rz}|_{z=0}=0, \tag{2}$$

and the initial values

$$\mathbf{U}|_{t=0}=\left.\frac{\partial\mathbf{U}}{\partial t}\right|_{t=0}=0, \tag{3}$$

where the following notation is used: $\mathbf{U}=\begin{pmatrix}U_r\\U_z\end{pmatrix}$ is the displacement vector, $\rho(z)$ is the density, $\lambda(z)$, $\mu(z)$ are Lamé's constants, E is the deformation tensor, the function $f(t)$ represents the time variation of the source, τ_{zz} and τ_{rz} are normal and tangential stresses, respectively.

(a) *The First Modification.* We seek a solution in the form of Fourier-Bessel integrals:

$$U_z=\int_0^\infty R(z,k,t)\,J_0(kr)\,dk, \tag{4}$$

$$U_r=\int_0^\infty S(z,k,t)\,J_1(kr)\,dk. \tag{5}$$

As a result, we obtain the following boundary value problem of reduced dimensionality for the functions $R(z, k, t)$ and $S(z, k, t)$:

0340-062X/80/0161/$02.40

$$\frac{\partial^2 \mathbf{G}}{\partial z^2} + A(z, k)\frac{\partial \mathbf{G}}{\partial z} + B(z, k)\,\mathbf{G} = C(z)\frac{\partial^2 \mathbf{G}}{\partial t^2}, \tag{6}$$

$$\left(\frac{\partial \mathbf{G}}{\partial z} + D(z, k)\,\mathbf{G}\right)\Big|_{z=0} = \varepsilon, \tag{7}$$

$$\mathbf{G}|_{t=0} = \frac{\partial \mathbf{G}}{\partial t}\Big|_{t=0} = 0, \tag{8}$$

where

$$\mathbf{G} = \begin{pmatrix} S(z, k, t) \\ R(z, k, t) \end{pmatrix}, \qquad \varepsilon = \begin{pmatrix} 0 \\ -kf(t) \end{pmatrix},$$

and A, B, C, D are known matrices. To solve this problem we use the method of finite differences. We must solve our problem for different values of k and then calculate the integrals (4) and (5) numerically. The system of Eqs. (6)-(8) must be solved for the values of k, which are knots of the quadrature formula, to allow the calculation of these integrals. If the values of k are small we can use an explicit scheme. Equation (6), in the form of an explicit scheme, enables us to compute the functions $R(z, k, t)$ and $S(z, k, t)$ at each spatial grid point, at the time step $(j+1)$, exclusively in terms of the values at the two previous time steps j and $(j-1)$. If the values of k are large, one has to use either a smaller time step Δt for the explicit scheme, or pass to an implicit scheme in order to make the computation stable.

The convergence of the Fourier-Bessel integrals is determined by the behaviour of the functions $R(z, k, t)$ and $S(z, k, t)$ as $k \to \infty$. For the case of an impulsive SH-torque source for a homogeneous model, we have analyzed the analytical solution for the boundary-value problem obtained after the separation of variables. The behaviour of $R(z, k, t)$ and $S(z, k, t)$ has been found to depend on the smoothness of the function $f(t)$ in the boundary condition. If $f(t)$ is a discontinuous function, one can speak of convergence of the integrals (4), (5) only in general terms. For smooth finite functions $f(t)$ the integrands $R(z, k, t)$ and $S(z, k, t)$ decrease exponentially as the parameter k increases, the integrals (4), (5) converge and therefore can be calculated numerically.

Replacing the integrals (4), (5) by those over a finite interval, we note that they are integrals of strongly oscillating functions. Therefore, to compute them we follow Filon's method: we consider $J_1(kr)$, $J_0(kr)$ as weight functions and substitute for $R(z, k, t)$ and $S(z, k, t)$ using an interpolation polynomial. Spline-interpolation of the second order is used.

The error in the method as a whole can be determined by comparison with the exact solution for the problem of an impulsive SH-torque source, for the case of a homogeneous model. The error in the displacement $U(r, z, t)$ does not exceed two or three per cent at distances up to $30\,\lambda_0$ (here λ_0 is the dominant wavelength radiated by the source). For details see Alekseev and Mikhailenko (1976), Mikhailenko (1973, 1974).

(b) *The Second Modification.* This method is based on combining finite-integral transformations (see Koshlyakov et al. 1970) with finite-difference methods. The use of finite-integral transformations considerably increases the possibilities of the method. Numerical integration of the rapidly-oscillating integrals (4), (5) is no longer necessary. To compute them one has only to solve a great number of one-dimensional problems at fixed values of the parameters k.

Consider problem (1)-(3) again and introduce new boundary conditions:

$$U_r(r, z, t)|_{r=r_0} = 0, \qquad U_z(r, z, t)|_{r=r_0} = 0. \tag{9}$$

We have thus introduced a reflecting surface at the distance $r = r_0$ from the origin. We select a sufficiently large distance r_0 and consider the wave field up to $t = T$, where T is the time taken for propagation of the wavefront up to the reflecting surface.

Let us apply finite Hankel integral transformations (see Sneddon 1951) along the coordinate r,

$$R_1(z, k_i, t) = \int_0^{r_0} r\,U_z(r, z, t)\,J_0(k_i r)\,dr, \tag{10}$$

$$S_1(z, \tilde{k}_i, t) = \int_0^{r_0} r\,U_r(r, z, t)\,J_1(\tilde{k}_i r)\,dr, \tag{11}$$

$$U_z(r, z, t) = \frac{2}{r_0^2}\sum_{i=1}^{\infty} R_1(z, k_i, t)\frac{J_0(k r_i)}{[J_1(r_0 k_i)]^2}, \tag{12}$$

$$U_r(r, z, t) = \frac{2}{r_0^2}\sum_{i=1}^{\infty} s_1(z, \tilde{k}_i, t)\frac{J_1(r\tilde{k}_i)}{[J_1'(r_0 \tilde{k}_i)]^2}, \tag{13}$$

where k_i are the roots of the equation $J_0(k_i r_0) = 0$, (14)

and $\tilde{k}_i$ are those of the equation $J_1(\tilde{k}_i r_0) = 0$. (15)

The boundary value problem of reduced dimensionality is:

$$\frac{\partial^2 \mathbf{Q}}{\partial z^2} + \tilde{A}(z, k_i^*)\frac{\partial \mathbf{Q}}{\partial z} + \tilde{B}(z, k_i)\,\mathbf{Q} = \tilde{C}(z)\frac{\partial^2 \mathbf{Q}}{\partial t^2}, \tag{16}$$

$$\frac{\partial \mathbf{Q}}{\partial z} + \tilde{D}(z, k_i^*)\,\mathbf{Q} = \tilde{\varepsilon} \quad \text{at} \quad z = 0, \tag{17}$$

$$\mathbf{Q}|_{t=0} = \frac{\partial \mathbf{Q}}{\partial t}\Big|_{t=0} = 0, \tag{18}$$

where $\mathbf{Q}(z, k_i^*, t)$ is the vector with the components $R_1(z, k_i, t)$ and $S(z, \tilde{k}_i, t)$, the coefficients $\tilde{A}$, $\tilde{B}$, $\tilde{C}$, $\tilde{D}$, $\tilde{\varepsilon}$ are known matrices, and the vector $k_i^* = \begin{pmatrix} k_i \\ \tilde{k}_i \end{pmatrix}$ contains the roots of Bessel's equations. Having solved problem (16)-(18) numerically for various roots of the Bessel's Eqs. (14), (15), we can find the components of the displacement vector by (12), (13).

The convergence of the series (12), (13) depends on the smoothness of the function $f(t)$. It can be shown that, if the function $f(t)$ satisfies the Dirichlet conditions, then as $k_i^* \to \infty$ the series converge rapidly. The above method allows one to calculate complete theoretical seismograms on the computer BESM-6 up to distances exceeding $100\,\lambda_0$ (λ_0 is the dominant wavelength generated by the source).

The total error in the determination of the displacement vector, caused by inaccuracy of the difference schemes and the truncation of the series, does not exceed 3 %-4 %. The method is easily generalized for anisotropic media. In this case only the coefficients in the difference equations are changed.

Other details can be found in Alekseev and Mikhailenko (1978).

2.2. Half-Space Inhomogeneous in the Horizontal Direction

Consider the application of the method to the calculation of wave fields in media where the elastic parameters are arbitrary functions of epicentral distance. In the system of Cartesian coordinates (x, z) propagation of SH waves from a line source is described by the equation

$$\frac{\partial}{\partial x}\left(\mu\frac{\partial U}{\partial x}\right)+\mu\frac{\partial^2 U}{\partial z^2}=\rho\frac{\partial^2 U}{\partial t^2}-\rho\,\delta(x)\,\delta(z-h)\,f(t), \tag{19}$$

with the boundary condition

$$\left.\frac{\partial U}{\partial z}\right|_{z=0}=0, \tag{20}$$

and the initial values

$$U|_{t=0}=\left.\frac{\partial U}{\partial t}\right|_{t=0}=0, \tag{21}$$

where $\mu(x)$ is Lamé's constant, and $\rho(x)$ is density.

For application of the finite integral transformation we introduce the boundary condition

$$\left.\frac{\partial U}{\partial z}\right|_{z=z_0}=0, \tag{22}$$

and select z_0 sufficiently far from the origin. The wave field is then considered up to the time $t=T$, where T is the time taken for wave propagation to the reflecting surface at $z=z_0$.

We employ the cosine transformation with finite limits

$$S(x,\eta,t)=\int_0^{z_0} U(x,z,t)\cos\frac{\eta\pi z}{z_0}\,dz, \tag{23}$$

$$U(x,z,t)=\frac{1}{z_0}S(x,0,t)+\frac{2}{z_0}\sum_{\eta=1}^{\infty} S(x,\eta,t)\cos\frac{\eta\pi z}{z_0}. \tag{24}$$

Multiplying Eq. (19) by $\cos\frac{\eta\pi z}{z_0}$ and integrating from zero to z_0, making use of conditions (20), (22), we obtain

$$\frac{\partial}{\partial x}\left(\mu\frac{\partial S}{\partial x}\right)-\mu\frac{\eta^2\pi^2}{z_0^2}S=\rho\frac{\partial^2 S}{\partial t^2}-\rho\,\delta(x)\cos\frac{\eta\pi h}{z_0}f(t), \tag{25}$$

$$S|_{t=0}=\left.\frac{\partial S}{\partial t}\right|_{t=0}=0. \tag{26}$$

Problem (25), (26) is solved by finite-difference methods for fixed values of η. Summing the values $S(x,\eta,t)$ for $\eta=0,1,2,\ldots,N$, according to formula (24), we find $U(x,z,t)$.

2.3. Radially Symmetric Medium

In the spherical system of coordinates r, Θ, φ

$(0<r\leqq a,\ 0\leqq\Theta\leqq\pi,\ 0\leqq\varphi\leqq 2\pi)$,

we consider a radially symmetric elastic medium where Lamé's constants λ, μ and density ρ are arbitrary, piecewise-continuous functions of the coordinate r. At the point $r=d$, $\Theta=0$, a vertical force is applied

$$\mathbf{F}=\delta(r-d)\frac{\delta(\Theta)}{d^2\sin\Theta}f(t)\,\mathbf{e}_r. \tag{27}$$

This force has axial symmetry and generates the displacement field

$$U=U_r(r,\Theta,t)\,\mathbf{e}_r+U_\Theta(r,\Theta,t)\,\mathbf{e}_\Theta. \tag{28}$$

The components $U_r(r,\Theta,t)$ and $U_\Theta(r,\Theta,t)$ are defined from the system of equations of the dynamic elasticity theory,

$$(\lambda+2\mu)\,\mathrm{grad}\,\mathrm{div}\,\mathbf{U}-\mu\,\mathrm{rot}\,\mathrm{rot}\,\mathbf{U}+\mathrm{div}\,\mathbf{U}\,\mathrm{grad}\,\lambda$$
$$+2(\mathrm{grad}\,\mu\cdot E)+\rho\mathbf{F}=\rho\frac{\partial^2\mathbf{U}}{\partial t^2}, \tag{29}$$

for zero initial values

$$\mathbf{U}|_{t=0}=\left.\frac{\partial\mathbf{U}}{\partial t}\right|_{t=0}=0, \tag{30}$$

and with boundary conditions at the free surface

$$\tau_{rr}|_{r=a}=0,\qquad \tau_{\Theta r}|_{r=a}=0, \tag{31}$$

where E is the deformation tensor, and τ_{rr}, $\tau_{\Theta r}$ are vertical and tangential stresses, respectively.

If, at the depth $r=d$, an impulsive SH-torque is applied

$$\mathbf{F}=2\,\delta(r-d)\frac{\delta(\Theta)}{d^3\sin^2\Theta}f(t)\,\mathbf{e}_\varphi, \tag{32}$$

then only SH-waves arise in the medium. The component $U_\varphi(r,\Theta,t)$ is determined from the equation

$$\frac{\mu}{r^2}\frac{\partial}{\partial\Theta}\left(\frac{\partial U_\varphi}{\partial\Theta}-U_\varphi\cot\Theta\right)+\frac{\partial}{\partial r}\left[\mu\left(\frac{\partial U_\varphi}{\partial r}-\frac{U_\varphi}{r}\right)\right]+3\frac{\mu}{r}\left(\frac{\partial U_\varphi}{\partial r}-\frac{U_\varphi}{r}\right)$$
$$+\frac{2\mu}{r^2}\left(\frac{\partial U_\varphi}{\partial\Theta}-U_\varphi\cot\Theta\right)\cot\Theta+\rho F=\rho\frac{\partial^2 U_\varphi}{\partial t^2}, \tag{33}$$

with the initial values

$$U_\varphi|_{t=0}=\left.\frac{\partial U_\varphi}{\partial t}\right|_{t=0}=0, \tag{34}$$

and the boundary condition at the free surface

$$\mu\left(\frac{\partial U_\varphi}{\partial r}-\frac{U_\varphi}{r}\right)\Big|_{r=a}=0. \tag{35}$$

If the Earth's core is liquid, then a similar boundary condition is introduced at the boundary of the core at $r=r_0$.

We seek a solution of Eqs. (29)–(31) in the form

$$U_r(r,\Theta,t)=\sum_{\eta=0}^{\infty} R(r,\eta,t)\,P_\eta(\cos\Theta), \tag{36}$$

$$U_\Theta(r,\Theta,t)=\sum_{\eta=0}^{\infty} S(r,\eta,t)\frac{\partial P_\eta(\cos\Theta)}{\partial\Theta}, \tag{37}$$

where the $P_\eta(\cos\Theta)$ are Legendre polynomials. To determine the functions $R(r, \eta, t)$ and $S(r, \eta, t)$ a new boundary value problem,

$$\frac{\partial}{\partial r}\left\{\lambda\left[\frac{\partial R}{\partial r}+\frac{2}{r}R-\frac{\eta(\eta+1)}{r}S\right]+2\mu\frac{\partial R}{\partial r}\right\}$$
$$+\frac{\mu}{r^2}\left\{4\frac{\partial R}{\partial r}r-4R+\eta(\eta+1)\left(3S-R-r\frac{\partial S}{\partial r}\right)\right\}+\rho F_r=\rho\frac{\partial^2 R}{\partial t^2}, \quad (38)$$

$$\frac{1}{r}\lambda\left[\frac{\partial R}{\partial r}+\frac{2}{r}R-\frac{\eta(\eta+1)}{r}S\right]+\frac{\partial}{\partial r}\left[\mu\left(\frac{\partial S}{\partial r}-\frac{S}{r}+\frac{R}{r}\right)\right]$$
$$+\frac{\mu}{r^2}\left[5R+3R\frac{\partial S}{\partial r}-S-2\eta(\eta+1)S\right]=\rho\frac{\partial^2 S}{\partial t^2}, \quad (39)$$

must be solved.

The boundary conditions at the free surface at $r=a$ are

$$(\lambda+2\mu)\frac{\partial R}{\partial r}+\frac{2\lambda}{r}R-\frac{\lambda}{r}\eta(\eta+1)S=0$$

and

$$\frac{\partial S}{\partial r}+\frac{1}{r}R-\frac{1}{r}S=0. \quad (40)$$

The initial conditions take the form

$$R|_{t=0}=\left.\frac{\partial R}{\partial t}\right|_{t=0}=0, \qquad S|_{t=0}=\left.\frac{\partial S}{\partial t}\right|_{t=0}=0. \quad (41)$$

Problem (38)–(41) is solved by finite-difference methods for different values of the parameter η which is the summation index in formulae (36), (37). We will not discuss the peculiarities of the numerical solution of problem (38)–(41); they are described in Alekseev and Mikhailenko (1977). Summing the functions $S(r, \eta, t)$ and $R(r, \eta, t)$ according to formulae (36), (37), we determine the displacement components $U_r(r, \Theta, t)$ and $U_\Theta(r, \Theta, t)$.

The number of terms of the series (36) and (37) depends on the smoothness of the function $f(t)$, i.e., on the frequency of the signal from the source. This number increases linearly with frequency. Theoretical seismograms for waves with periods longer than 5–10 s can be calculated on the computer BESM-6. For other details see Alekseev and Mikhailenko (1977).

2.4. *Diffraction by a Wedge in an Inhomogeneous Medium*

In a cylindrical system of coordinates $0\leqq r<\alpha$, $0\leqq\varphi<2\pi$, consider the wave equation with the variable velocity $v_p(r)$ and a line source located outside a wedge, at the point (r_0, φ_0):

$$\frac{\partial^2 U}{\partial r^2}+\frac{1}{r}\frac{\partial U}{\partial r}+\frac{1}{r^2}\frac{\partial^2 U}{\partial\varphi^2}$$
$$=\frac{1}{v_p^2(r)}\frac{\partial^2 U}{\partial t^2}-\frac{2\pi}{r_0}\delta(\varphi-\varphi_0)\,\delta(r-r_0)\,f(t). \quad (42)$$

On the boundaries of the wedge the conditions

$$U|_{\varphi=0}=0, \qquad U|_{\varphi=\alpha}=0, \quad (43)$$

are fulfilled, where α is the angle of the wedge ($\pi<\alpha<2\pi$). The initial values are

$$U|_{t=0}=0, \qquad \left.\frac{\partial U}{\partial t}\right|_{t=0}=0. \quad (44)$$

Applying the sine transformation with finite limits,

$$R(r, \eta, t)=\int_0^\alpha U(r, \varphi, t)\sin\frac{\eta\pi\varphi}{\alpha}\,d\varphi, \quad (45)$$

$$U(r, \varphi, t)=\frac{2}{\alpha}\sum_{\eta=1}^{\infty}R(r, \eta, t)\sin\frac{\eta\pi\varphi}{\alpha}, \quad (46)$$

we obtain a new problem

$$\frac{\partial^2 R}{\partial r^2}+\frac{1}{r}\frac{\partial R}{\partial r}-\frac{\eta^2\pi^2}{r^2\alpha^2}R=\frac{1}{v_p^2(r)}\frac{\partial^2 R}{\partial t^2}-\frac{4\pi}{r_0}\sin\frac{\eta\pi\varphi}{\alpha}\delta(r-r_0)\,f(t), \quad (47)$$

$$R|_{t=0}=\left.\frac{\partial R}{\partial t}\right|_{t=0}=0. \quad (48)$$

Problem (47), (48) is solved by finite-difference methods at fixed values of η. The displacement $U(r, \varphi, t)$ is then found from (46). If the boundary conditions on the sides of the wedge are of the form

$$\left.\frac{\partial U}{\partial r}\right|_{\varphi=0}=0, \qquad \left.\frac{\partial U}{\partial r}\right|_{\varphi=\alpha}=0, \quad (49)$$

then a cosine transformation with finite limits is applied.

Changing the velocity and the angle of the wedge, sufficiently complicated models of the media can be obtained.

2.5. *Other Diffraction Problems: Block Structures*

Without significant modifications the method is applied both to diffraction by a cylinder in an inhomogeneous medium and diffraction of a spherical wave by an opaque cone. In the first case we use the Fourier series with respect to the angular coordinate $\varphi(0\leqq r<\infty, 0\leqq\varphi<2\pi)$; in the second case the finite-integral Legendre transformation with respect to the angular coordinate $\Theta(0\leqq r<\infty, 0\leqq\Theta<\alpha)$ is used.

Employing finite transformations within the limits 0 to a and b, and connecting the solutions with the help of the finite-difference method, one can solve problems for inhomogeneous media with block structure, each block having its own parameters $\lambda(z)$, $\mu(z)$ and density $\rho(z)$.

At present, the method has been applied to construct theoretical seismograms for certain types of visco-elastic media, porous media and pre-stressed media. If Lamé's constants λ, μ and density ρ are arbitrary functions of some space variables, the classical separation of variables does not take place. In this case, employing finite integral transformations can be suggested as a rather effective method for calculation of theoretical seismograms (Mikhailenko 1978, 1979).

3. Certain Dynamical Peculiarities of Seismic Waves in Inhomogeneous Media: Non-Ray Effects

In this section, we will present examples of computations of theoretical seismograms for some simple models. These examples are not of methodological character, but they demonstrate

certain results which are of great interest in seismology and in seismic prospecting.

In all the examples presented, we consider a source with a source time function $f(t)$ given by the formula:

$$f(t)=\begin{cases} C\cdot[\sin(2\pi t/T)-0.5\sin(4\pi t/T)], & 0\leqq t\leqq T, \\ 0, & t<0,\ t>T. \end{cases} \tag{50}$$

3.1. *Vertically Inhomogeneous Media*

First Example. First we will consider a classical seismological model: a homogeneous layer overlaying a homogeneous halfspace, with a point source located at arbitrary depth (see Fig. 1). We select an explosive-type source, with unidirectional radiation characteristic. The parameters of the model under consideration are as follows:

$v_{p1}/v_{p2}=0.5$, $v_{s1}/v_{s2}=0.5$, $\rho_1/\rho_2=0.8$. The source is located at a depth of 2 km, the interface at a depth of 3 km. A number of papers have been devoted to this problem. For example, Alterman and Karal (1968) have solved this problem by the method of finite differences (with explicit schemes).

The theoretical seismograms of horizontal displacement U_r and vertical displacement U_z for six distances are shown in Fig. 2.

An interesting effect can be observed in Fig. 2, in the theoretical seismograms of the vertical component U_z, for the epicentral distance $R=0$. According to geometric ray theory the converted *PS* wave (reflected from the interface between the layer and the halfspace) should vanish for $R=0$. In Fig. 2, however, the *PS* wave following the *PP* wave can be seen clearly, even for $R=0$. The amplitude of the *PS* wave at $R=0$ depends on the distance of the source from the interface and on the elastic parameters of both media. The form of the *PS* wave at $R=0$ is the integral of the incident *P*-signal. As the epicentral distance increases, the form of the *PS* wave changes successively; at larger epicentral distances it is the same as the form of the *PP* wave, with opposite polarity. Note that the source time-function, given by $f(t)$, is differentiated in the explosive-type source). It should be noted that, for the source depth chosen (about 2 wavelengths), the Rayleigh wave is too weak to be seen in the seismograms.

Second Example. In this example, we consider a homogeneous halfspace with a free surface. A point source of the vertical-force type is located at a depth of 2 km. Two waves are seen clearly in the seismograms (Fig. 3) – the *P* wave, immediately followed by the *S* wave. The pulse shape of the vertical component of the *S* wave is the integral of $f(t)$ at small epicentral distances and changes successively to $f(t)$ as the epicentral distance increases. For angles of incidence larger than $\Theta=\sin^{-1}(v_s/v_p)$, the *S* wave changes its polarization from linear to elliptic.

Third Example. In this example, we consider a high-velocity layer located in a homogeneous halfspace (see Fig. 4). We consider a point *SH*-torque source located at the free surface. The wave field connected with high-velocity layers has a number of interesting peculiarities. A considerable amount of attention has been devoted by various authors to the so-called 'interference head waves' and to the 'tunnel waves'. It is of great importance to investigate the properties of these waves as a function of l/λ_2 (where l is the thickness of the layer and λ_2 the wavelength within the layer).

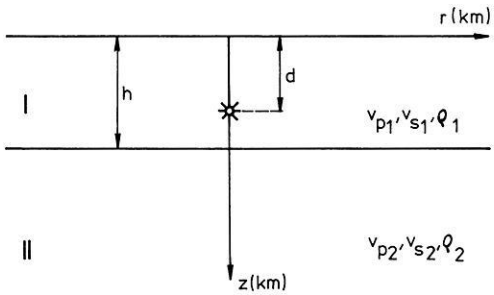

Fig. 1. Layered halfspace with an explosive point source

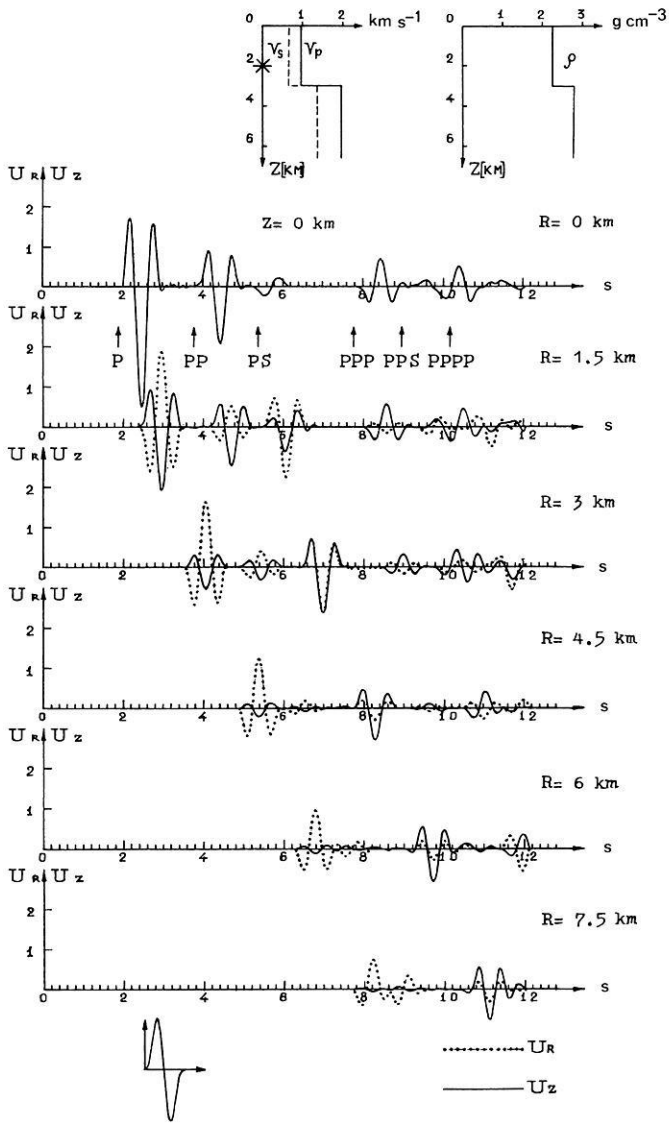

Fig. 2. Horizontal and vertical displacements U_r *(dotted curve)* and U_z *(solid curve)* on the surface of a layered halfspace ($z=0$) for different epicentral distances R. A point source of explosive type is located at a depth of 2 km, the interface at a depth of 3 km ($v_{p1}/v_{p2}=0.5$, $v_{s1}/v_{s2}=0.5$, $\rho_1/\rho_2=0.8$). The source time-function with a duration of 1 s is shown at the bottom-left. At the top are shown *P* and *S* wave velocity-depth graphs and the density-depth graph for the model used for computations

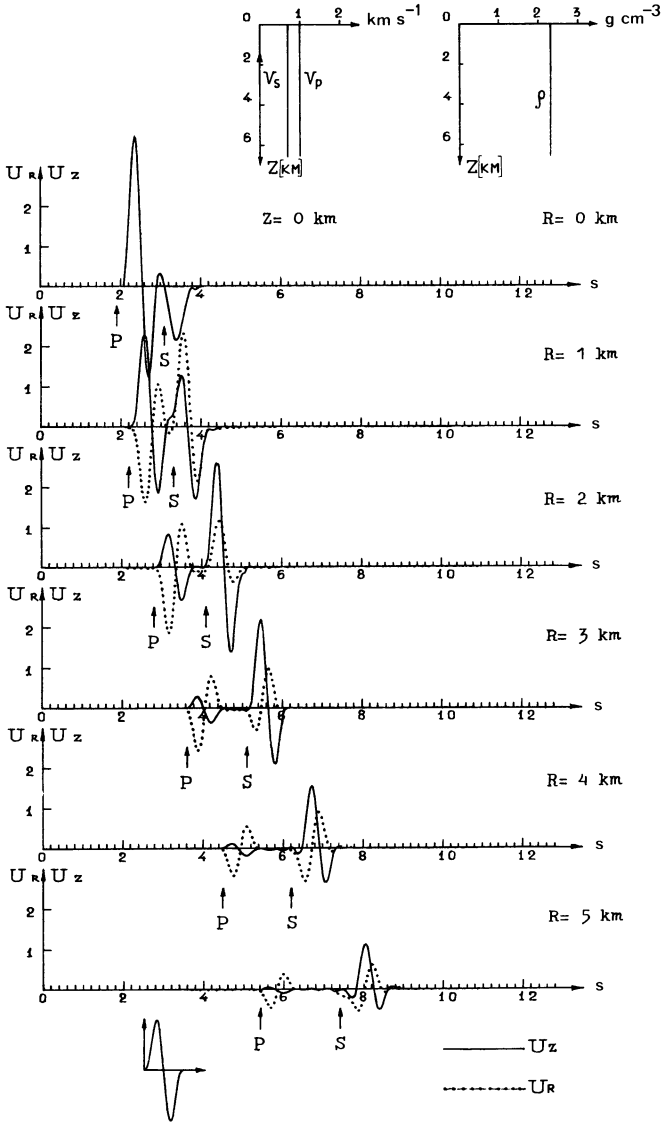

Fig. 3. Horizontal and vertical displacements U_r *(dotted curve)* and U_z *(solid curve)* on the surface of a homogeneous halfspace ($z=0$) for different epicentral distances R. An impulsive vertical-force point-source is located at a depth of 2 km. The source time-function with a duration of 1 s is shown at the bottom-left. At the top are shown P and S wave velocity-depth graphs and the density-depth graph for the model used for computations

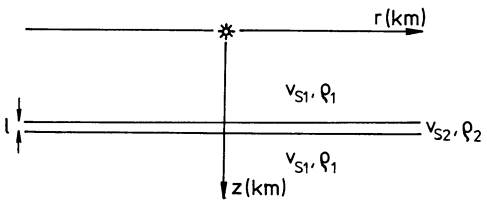

Fig. 4. Thin layer embedded in a halfspace model of Fig. 4

The process generating the interference head-wave along a thin high-velocity layer is closely connected with the interference group of multiply-reflected waves propagating within the layer. This interference group of multiply-reflected waves forms a distinct wave. Computations show that the amplitudes of interference head-waves depend not only on l/λ_2, but also on the velocities inside and outside the layer. For a larger velocity change (say, $v_{s1}/v_{s2}=0.5$), the maximum amplitudes have been observed for $l/\lambda_2 \sim 0.1$. The velocity of propagation of the interference head-wave is approximately 6%–7% lower than the velocity of head-wave propagation along an interface between two halfspaces. For a smaller velocity change ($v_{s1}/v_{s2}>0.7$) the amplitudes of interference head-waves decrease with decreasing l/λ_2. The change of velocity is not observed in this case.

Another interesting non-ray wave, connected with the high-velocity layer, is the tunnel wave (also called the screened wave). The generation of the tunnel wave cannot be explained by ray theory, it does not propagate through the layer along a ray-path,

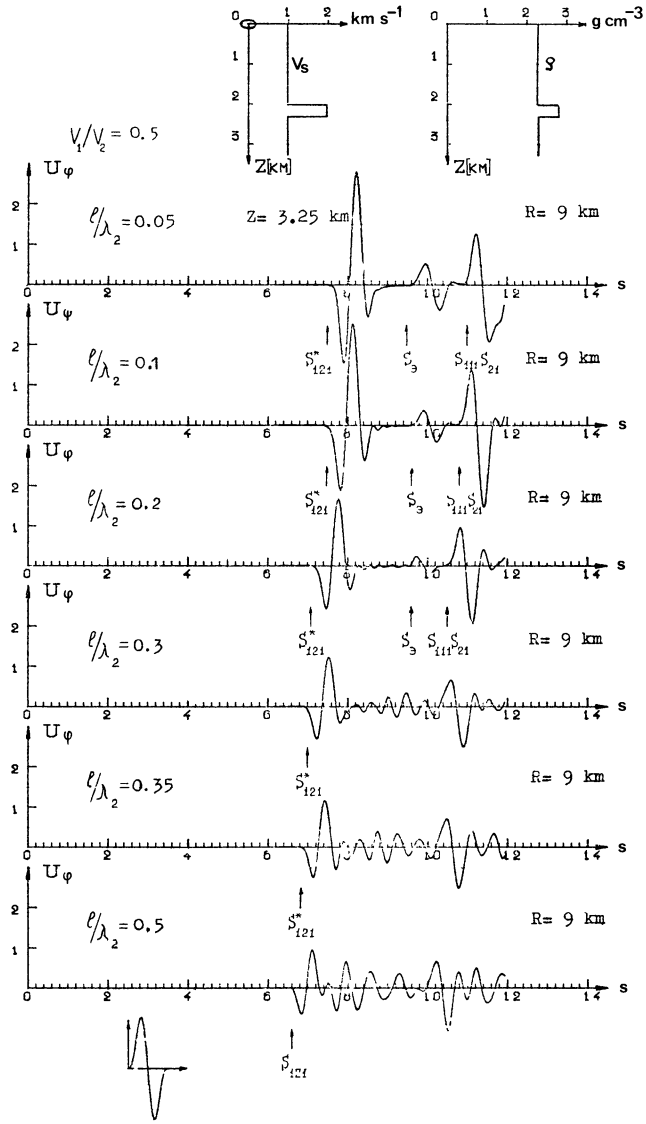

Fig. 5. Horizontal displacement U within the model of Fig. 4 a depth of 3.25 km and at the epicentral distance 9 km for different l/λ_2, where l is the thickness of the layer and λ_2 is the wavelength within the layer. A point SH-torque source is located at the free surface. The source time-function with a duration of 1 s is shown at the bottom-left.
At the top are shown S wave velocity-depth and density-depth graphs for the model used for computations

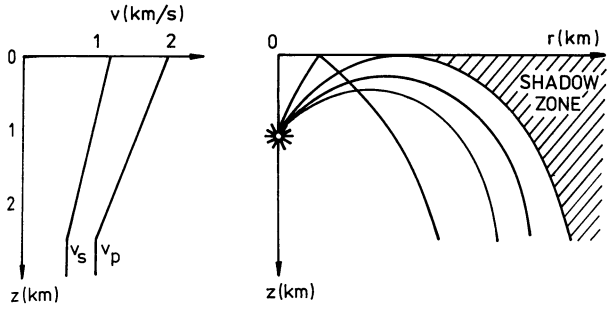

Fig. 6. Model of an anti-waveguide and corresponding rays

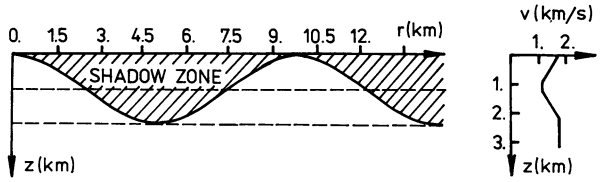

Fig. 8. Model of a waveguide and corresponding limiting ray

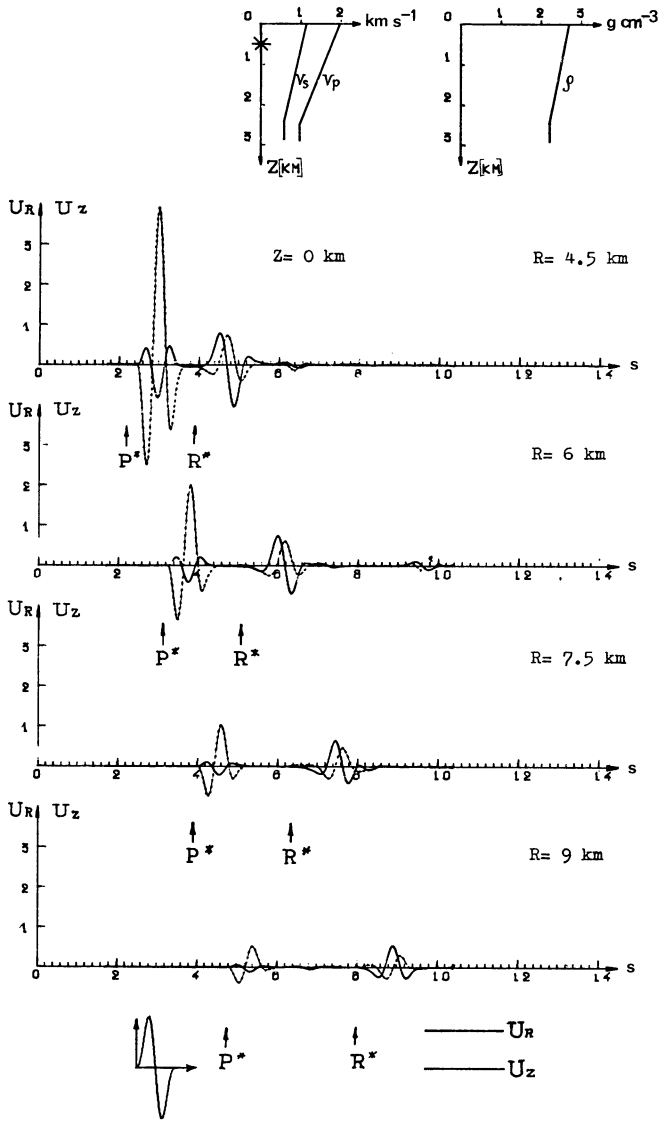

Fig. 7. Horizontal and vertical displacements U_r *(dotted curve)* and U_z *(solid curve)* at the surface of an inhomogeneous half-space (Fig. 6) for different epicentral distances R. An explosive-type point-source is located within the inhomogeneous anti-waveguide at a depth of 1 km. The source time-function with a duration of 1 s is shown at the bottom-left.
At the top are shown P and S wave velocity-depth graphs and the density-depth graph for the model used for computations

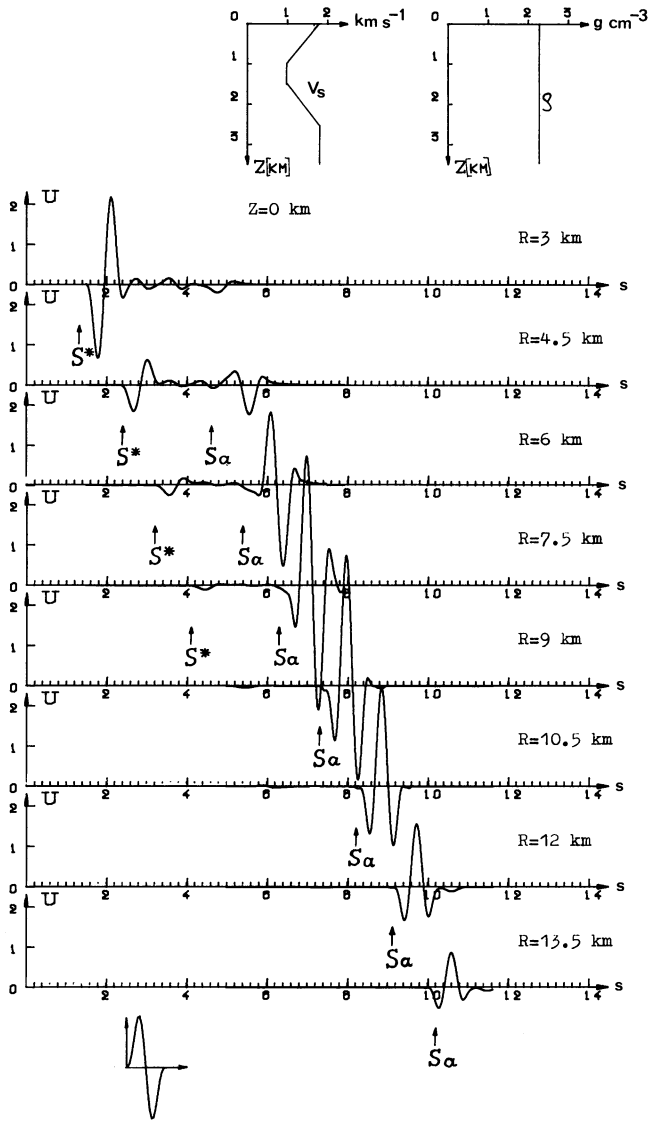

Fig. 9. Horizontal displacement U_φ at the free surface of the waveguide (Fig. 8) for different epicentral distances R. A point SH-torque source is located at the free surface. S_a is a channel wave. The source time-function with a duration of 1 s is shown at the bottom-left. At the top are shown S wave velocity-depth and density-depth graphs for the model used for computations

it 'tunnells'. Only lower frequencies are tunnelled, higher frequencies are screened. Thus, the dominant frequencies of the tunnel wave decrease. The amplitudes of tunnel waves depend on l/λ_2; they decrease with increasing l/λ_2.

Theoretical seismograms for various values of l/λ_2, for the epicentral distance $R=9$ km are shown in Fig. 5. The source is

located on the free surface, the receiver, at a depth of 3.25 km below the high-velocity layer ($v_{s1}/v_{s2}=0.5$). The wave observed as the first arrival (S^*_{121}) is the interference head wave. The tunnel wave S_3 does not have a distinct onset, its pulse shape corresponds approximately to the integral of the incident pulse.

Fourth Example. Now we will consider a model with an anti-waveguide (see Fig. 6). A point source of explosive type is located within the inhomogeneous anti-waveguide, at a depth of 1 km. Theoretical seismograms for four epicentral distances in the shadow zone are shown in Fig. 7. The wave reflected from

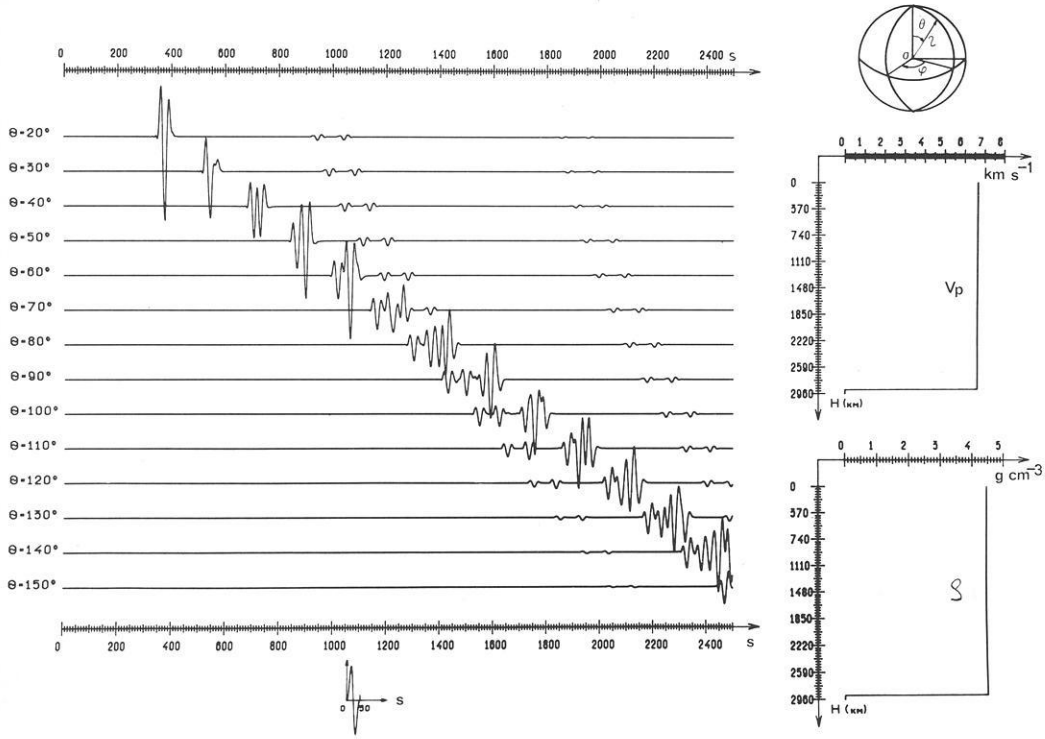

Fig. 10. Theoretical seismograms for a homogeneous spherical Earth model ($v_s=6.24$ km/s, $\rho=4.46$ g/cm^3) with a liquid core for different epicentral distances θ. A torque-type source is located at a depth of 300 km and generates a pulse with a duration of 50 s. The source time-function is shown at the bottom-left. At the right-hand side are P wave velocity-depth (*top*) and density-depth (*bottom*) graphs for the model used for computations

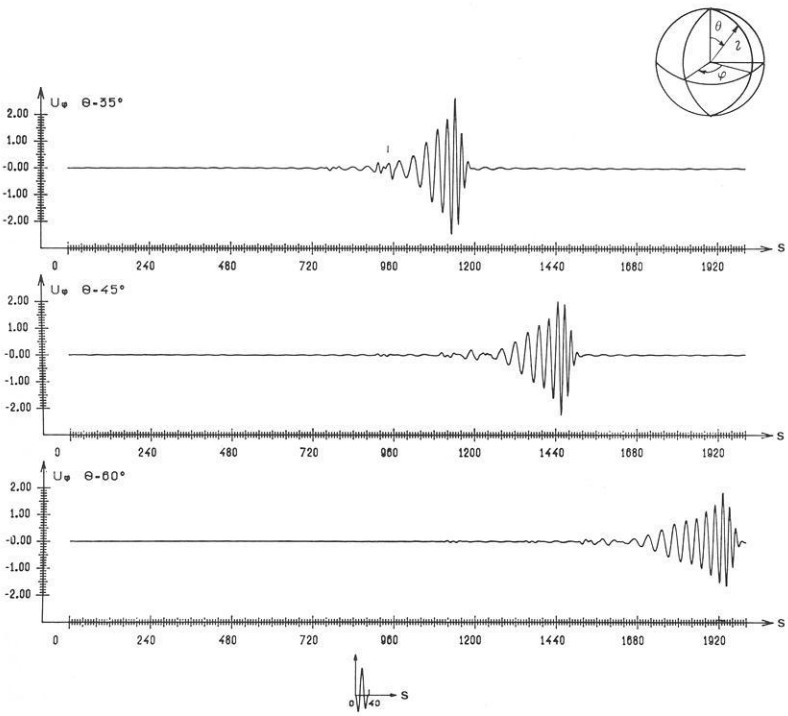

Fig. 11. Theoretical seismograms for the Gutenberg model for different epicentral distances Θ. A torque-type source is located at a depth of 28 km and generates a pulse with a duration of 40 s. The source time-function is shown at the bottom-left

the interface of the second order at the depth of 2.5 km is very weak. As shown in Fig. 7, the shape of the diffracted wave P^* changes with increasing epicentral distance. The amplitude spectrum of the diffracted wave is shifted to lower frequencies. The prevailing frequency of the diffracted wave is about 30% lower than the prevailing frequency of the direct wave in the illuminated region. In Fig. 7, one can also observe the Rayleigh wave (denoted by R^*). The displacement vector of the R^* wave rotates in the rz plane. This rotation can be seen clearly in Fig. 7.

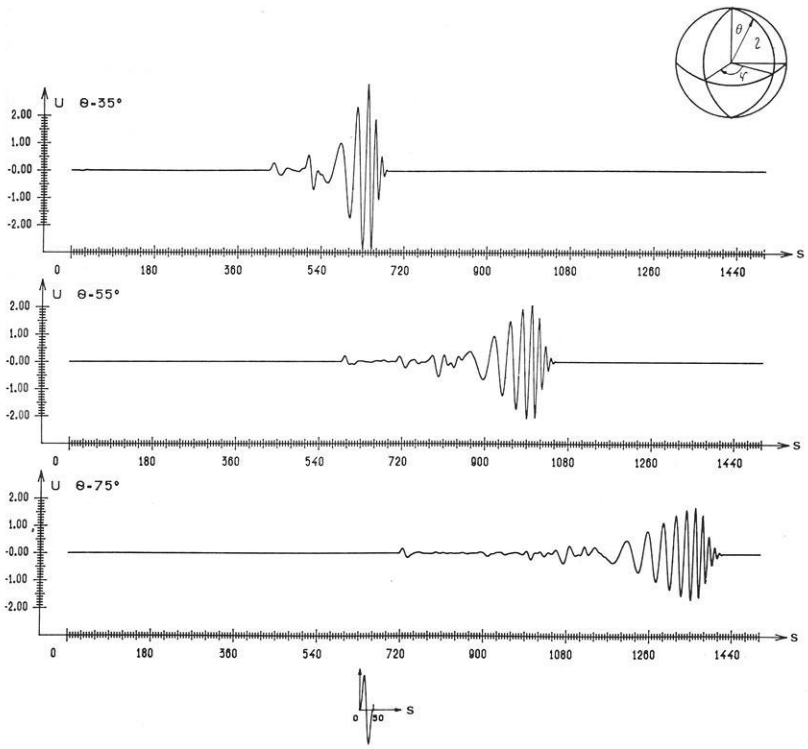

Fig. 12. Theoretical seismograms of P waves for a liquid Earth model similar to the Jeffreys-Bullen model for different epicentral distances Θ. An explosive-type source is located at the free surface and generates a pulse with a duration of 30 s. The source time-function is shown at the bottom-left

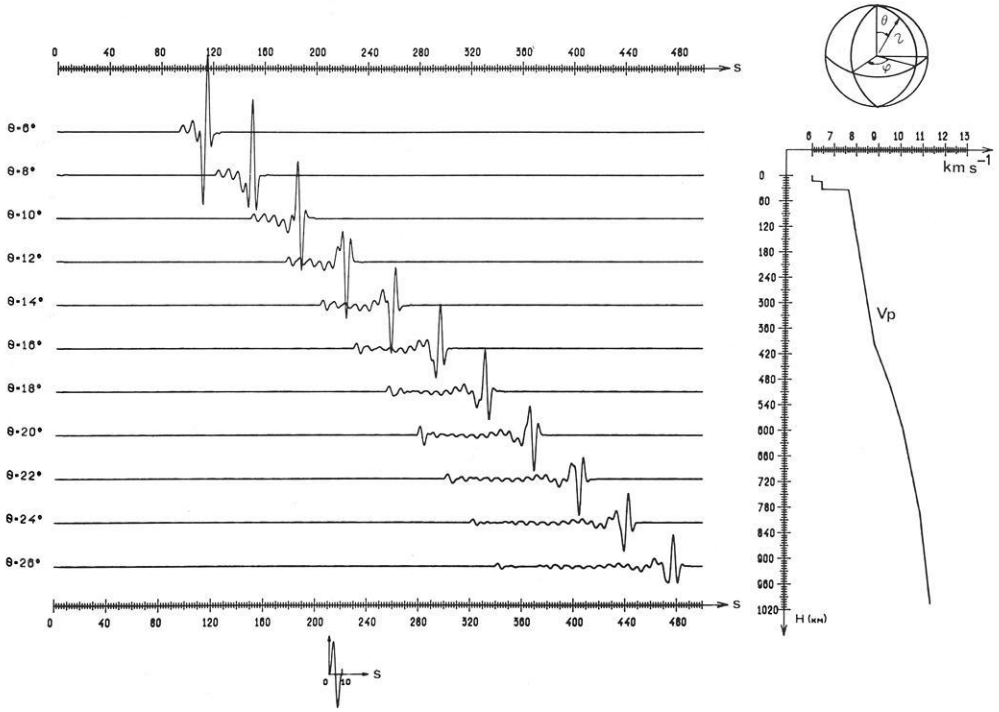

Fig. 13. Theoretical seismograms of P waves for a liquid Jeffreys-Bullen model for different epicentral distances θ. An explosive-type source is located at the free surface and generates a pulse with a duration of 10 s. The source time-function is shown at the bottom-left. At the right-hand side is a P wave velocity-depth graph for the model used for computations

Fifth Example. Now we will consider a symmetrical sub-surface waveguide. The model and corresponding rays are shown in Fig. 8. The source radiates *SH* waves and is located on the free surface. For this model large shadow-zones are formed on the free surface. The shadow zones are separated by illuminated regions or by regions where rays are focussed. The zones of maximum energy correspond to regions where the boundary rays touch the free surface (see Fig. 8). Theoretical seismograms for this model are shown in Fig. 9. The characteristic peculiarity of these seismograms is the disappearance of first arrivals and the increase in amplitudes of second arrivals, S_a (the channel waves).

3.2. Radially Symmetric Medium

First Example. We consider a homogeneous spherical Earth model ($v_s = 6.24$ km/s, $\rho = 4.46$ g/cm^3) with a liquid core. A torque-type source is located at a depth of 300 km and generates a pulse with a period $T = 50$ s. The corresponding theoretical seismograms, at the Earth's surface, for epicentral distances from $\Theta = 20°$ to $\Theta = 150°$ are shown in Fig. 10.

Second Example. In Fig. 11, theoretical seismograms are given for the Earth's surface for epicentral distances of 35°, 45°, and 60° for the Gutenberg model. A torque-type source is located at a depth of 28 km and generates a pulse with a period of 40 s. The amplitudes of the direct *SH* waves are small compared to those of the Love wave and hence are not well seen in the seismograms.

Third Example. In Fig. 12, theoretical seismograms of *P* waves are presented for the Earth's surface for epicentral distances of 35°, 45°, and 60° for an Earth model similar to the Jeffreys-Bullen model. An explosion-type source is located at the free surface and generates a pulse with a period of 30 s. The mantle-refracted wave is recorded as the first arrival.

Fourth Example. In Fig. 13 theoretical seismograms of *P* waves are presented for epicentral distances from 6° to 26° for the Jeffreys-Bullen model. An explosion-type source is located at the free surface and generates a pulse with a period of 10 s. In the Jeffreys-Bullen model the refracted wave is clearly distinguished as the first arrival for all distances. This wave has maximum amplitudes at 20°.

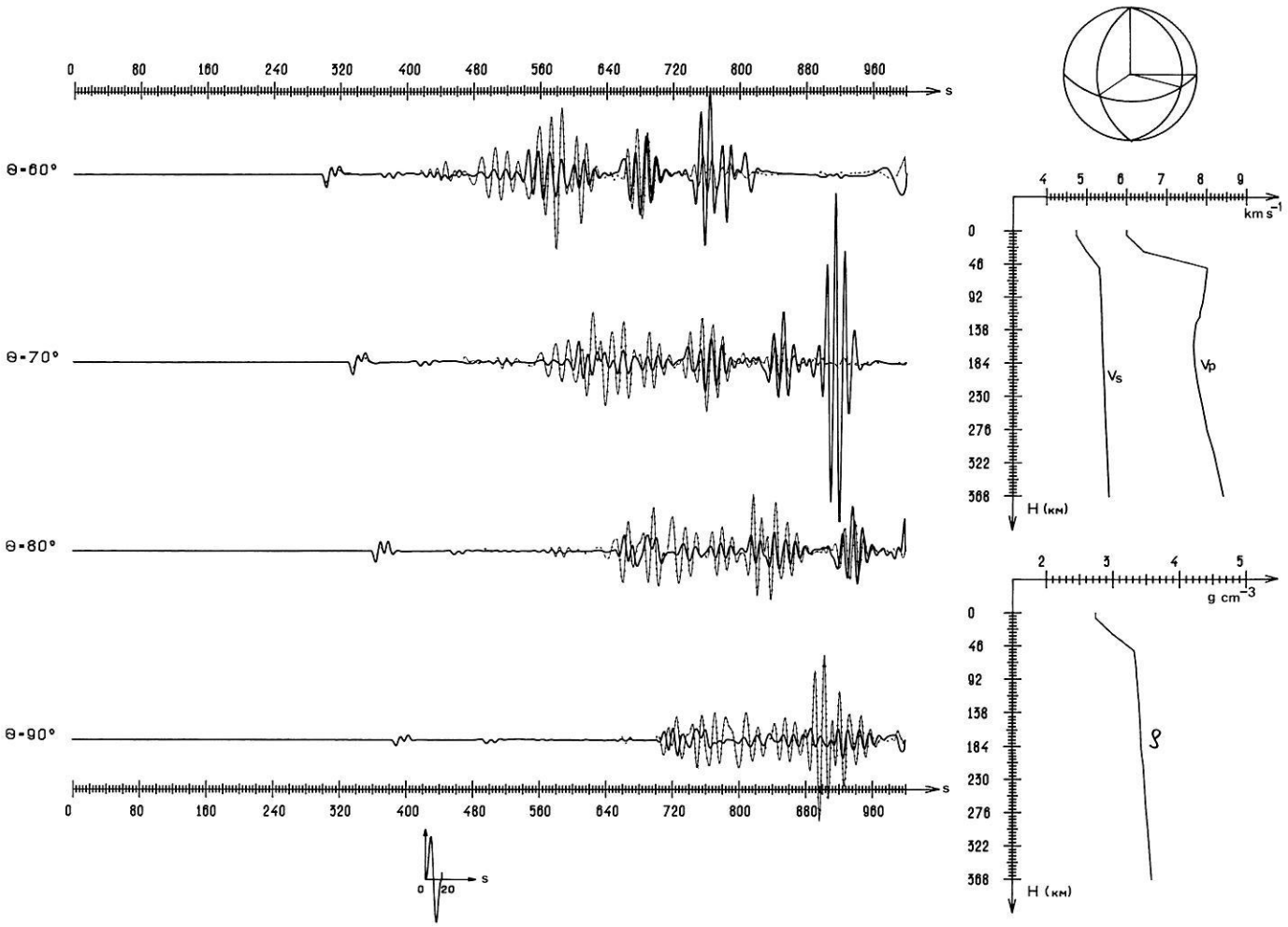

Fig. 14. Theoretical seismograms for the components U_r (*solid curve*) and U_Θ (*dotted curve*) at the free surface of the model on the right for different epicentral distances θ. A vertical-force-type source is located at a depth of about 60 km and generates a pulse with duration of 20 s. The source time-function is shown at the bottom-left. At the right-hand side are *P* and *S* wave velocity-depth graphs (*top*) and density-depth graph (*bottom*) for the model used for computations

In Fig. 14 theoretical seismograms are presented for epicentral distances of 60°, 70°, 80°, and 90° for a vertical-force-type source located at a depth of about 60 km, generating a pulse with a period of 20 s.

3.3. *Diffraction by a Wedge and a Cylinder*

First Example. In Fig. 15, theoretical seismograms for the diffraction of a cylindrical wave by a wedge are presented. An explosion-type source is located at the point ($z=2\lambda$, $\varphi_0=45°$) where λ is the dominant wavelength. The seismograms have been computed for 10 points located on a semicircle with radius $R=2\lambda$ at angular intervals of 20°, beginning with 90° (the first point). The angle of the wedge is $\alpha=315°$.

Second Example. In Fig. 16, the computed wave-field for the diffraction of a cylindrical wave by a cylinder is presented. An explosion-type source is located at the point $d=5\lambda$. The three-dimensional representation of the wave field is constructed in the square abcd outside the cylinder, for a certain instant of time. As can be seen, focussing of the wave-field takes place within the limits ab, as the velocity in the cylinder is less than that outside.

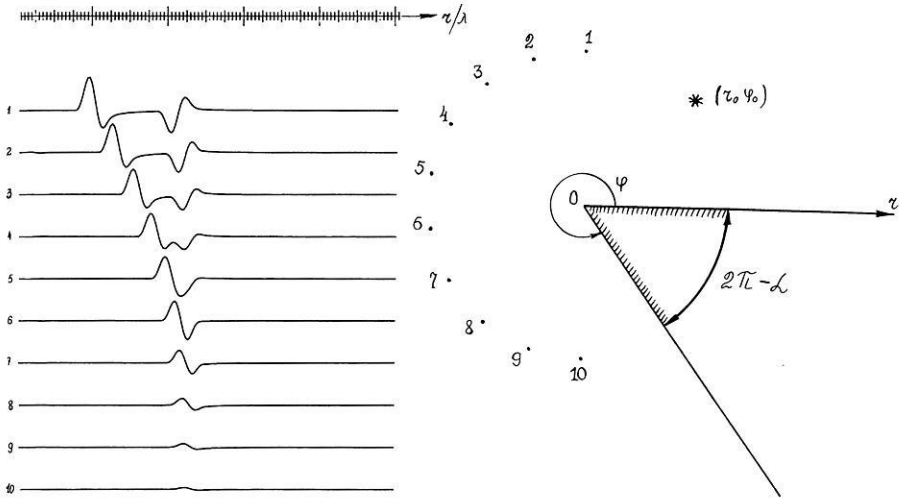

Fig. 15. Theoretical seismograms for 10 points located on a semicircle with radius 2λ (λ is the dominant wavelength) for the diffraction of a cylindrical wave by a wedge. The angle α of the wedge is 305°. The source is located at the point denoted by the asterisk

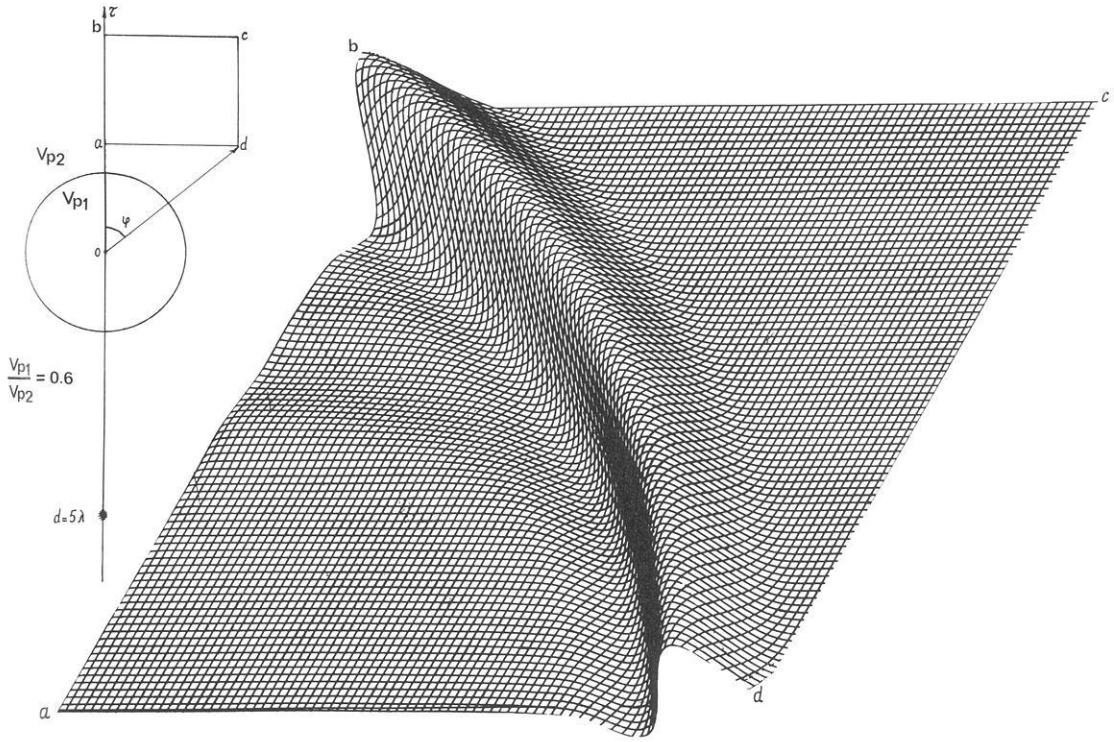

Fig. 16. Three-dimensional wave-field constructed in the square abcd for a certain instant of time, for the diffraction of a cylindrical wave by a cylinder. A explosive-type source is located outside the cylinder at the point 5λ

Conclusion

The method suggested has some advantages compared to known methods of calculation of theoretical seismograms. It does not require large amounts of computer store and is much more efficient and accurate than ordinary finite-difference methods, applicable to the solution of plane and axially-symmetric elasticity-theory problems with coefficients dependent on one space variable. It is not very difficult to apply the method to the calculation of theoretical seismograms for inhomogeneous, anisotropic, viscoelastic media as well as to porous and prestressed media, complete theoretical seismograms being computed in each case.

At present the method has been developed further for the calculation of theoretical seismograms for media whose parameters are arbitrary functions of two or three space variables.

References

Alekseev, A.S., Mikhailenko, B.G.: The solution of Lamb's problem for a vertically inhomogeneous elastic half-space. Izv. Akad. Nauk SSSR, Fiz. Zemli **12**, 11–25, 1976

Alekseev, A.S., Mikhailenko, B.G.: Numerical modelling of seismic waves propagating in a radially inhomogeneous Earth's model. Dokl. Akad. Nauk SSSR **235**, 46–49, 1977

Alekseev, A.S., Mikhailenko, B.G.: The method of calculation of theoretical seismograms for complex media models. Dokl. Akad. Nauk SSSR **240**, 1062–1065, 1978

Alterman, Z., Karal, F.C.: Propagation of elastic waves in layered media by finite difference methods. Bull. Seismol. Soc. Am. **58**, 367–398, 1968

Červený, V., Molotkov, I.A., Pšenčík, I.: Ray method in seismology. Univerzita Karlova: Praha, 1977

Koshlyakov, N.S., Gliner, E.B., Smirnov, M.M.: Partial differential equations of mathematical physics. Moscow: Vysshaya shkola 1970

Mikhailenko, B.G.: Numerical solution of Lamb's problem for inhomogeneous half-space. In: Mathematical problems of geophysics, Vol. 4, M.M. Lavrentiev and A.S. Alekseev, eds: pp. 273–297. Novosibirsk: Computing Center Acad. Sci. USSR (Sib. Division) 1973

Mikhailenko, B.G.: Numerical simulation of elastic wave propagation in the thin layer. In: Mathematical problems of geophysics, Vol. 5/1, M.M. Lavrentiev and A.S. Alekseev, eds.: pp. 187–194. Novosibirsk: Computing Center Acad. Sci. USSR (Sib. Division) 1974

Mikhailenko, B.G.: Calculation of theoretical seismograms for multi-dimensional medium models. In: Uslovno-korrektnye zadachi matematicheskoy fiziki v interpretatsii geofizicheskikh nablyudenii. Izd. VTs SO AN USSR 1978

Mikhailenko, B.G.: The method of solution of dynamic seismic problems for two-dimensional inhomogeneous media models. Dokl. Acad. Nauk USSR **246**, 47–51, 1979

Sneddon, I.: Fourier transforms. New York, Toronto, London 1951

Received August 1, 1978; Revised Version July 15, 1979
Accepted March 17, 1980